

# High-Speed Computation of Single and Coupled Microstrip Parameters Including Dispersion, High-Order Modes, Loss and Finite Strip Thickness

ROLF H. JANSEN, MEMBER, IEEE

**Abstract**—Based on an optimized rigorous hybrid mode solution for covered/open zero thickness microstrip patterns the following frequency dependent single and coupled line data are evaluated with very short CP-times: The characteristic impedances of the even and odd quasi-TEM modes, the propagation/attenuation constants and associated strip current density components of these and the higher order modes, the loss of the dominant modes under consideration of nonuniform strip current, substrate surface roughness and dielectric loss tangent. Finite strip thickness is introduced by a correction of the strip width input values.

## INTRODUCTION

DURING the last years the use of microstrip lines in microwave integrated circuits has been characterized by two interdependent developments. On the one hand, practical applications have been extended to higher frequencies in order to fully exploit the technological advantages of microstrip. This means an extension of the range of use to nonstatic conditions and requires that the frequency dependent line properties can be predicted precisely, especially in broadband design. Therefore, on the theoretical side of research an increased activity has been directed towards the finding of rigorous numerically efficient hybrid mode solutions for the associated boundary-value problems. The results of these efforts are documented by many publications, whereof, however, only those shall be referenced here which employ a one-dimensional formulation in terms of the strip surface current density and typically result in low matrix orders for a given prescribed accuracy, i.e., in low numerical expense [1]–[12]. In addition, the solutions referred to are exact in the sense that convergence to any desired degree of output data accuracy can be studied. Recent publications by Yamashita and Atsuki [11] and by Farrar and Adams [12] show that the subject under discussion is still of considerable interest. However, up to now computations like those cited above are still widely regarded as too laborious to compete with quasi-static formulas for effective dielectric constants, characteristic impedances and loss. One of the reasons for this might be that in the recent papers no design parameters beyond propagation constants are reported at all, though these should be available from the

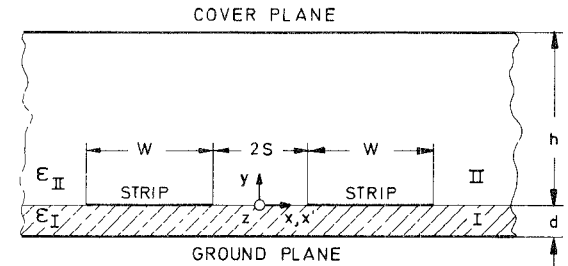


Fig. 1. Representative covered microstrip coupled line geometry.

computations with little additional effort. Instead, designers must make do with approximate results, for example, [13], which are achieved under the assumption of a uniform purely longitudinal current distribution and the accuracy of which can only be estimated. Therefore, it is one of the goals of this paper to demonstrate how the frequency dependent properties of single and coupled microstrip lines can be calculated rigorously, accurately and with further reduced computer time and storage requirements. Next, for lines fabricated on the most commonly used 25-mils alumina substrate extensive numerical results shall be presented as an aid in broad-band design.

## COMPUTATIONAL PROCEDURE

The real symmetrical integral eigenvalue equation which governs the behavior of propagation and attenuation modes ( $z$ -dependence  $\exp(-\gamma z)$ ) on covered microstrip patterns as represented by the cross sectional structure in Fig. 1 has been described in detail before [10]. Its derivation will, therefore, not be repeated. Strictly speaking, it is just the mathematically formulated requirement that the electrical field  $\bar{E}_t$  tangential to the infinitely thin conducting strip pattern should vanish by suitable selection of the longitudinal and transverse surface current density components  $\bar{J}_z$  and  $\bar{J}_x$  existing thereon, namely

$$\begin{aligned} \bar{E}_t &= \frac{1}{2\pi} \int_0^\infty \int_0^\infty \left( Z_{xx}(k_x) f_0 f'_0 Z_{xz}(k_x) f_0 f'_E \right) \left( \bar{J}_x(x') \right) \left( \bar{J}_z(x') \right) dx' dk_x \\ &= \begin{pmatrix} \bar{E}_x(x) \\ \bar{E}_z(x) \end{pmatrix} \equiv 0 \end{aligned} \quad (1)$$

with  $x$  and nonzero contributions from  $x'$  on the strips. The

Manuscript received March 18, 1977; revised May 27, 1977.

The author is with the Institut für Hochfrequenztechnik, Technical University of Aachen, Aachen, Germany.

abbreviations  $f_0 \cdots f'_E$  denote sine and cosine functions of argument  $k_x \cdot x$  and  $k_x \cdot x'$  where  $k_x$  is the separation constant with respect to the  $x$  direction. Their special arrangement in (1) describes the even case, i.e., with a magnetic wall at  $x = 0$ , whereas for the odd case the subscripts 0 and  $E$  must be interchanged and the sign of  $Z_{xz}$  be altered. Asymmetric problems can be solved by forming a composite integral equation which contains even and odd terms [14].

The above formulation is entirely real and symmetrical for both propagation and attenuation modes. This is a good starting point for an optimal computer implementation and reduces CP-time requirements *a priori*. It is achieved by the normalizations [10]

$$\begin{aligned} \begin{pmatrix} \bar{E}_x(x) \\ \bar{E}_z(x) \end{pmatrix} &= \begin{pmatrix} -E_x^I(x) \\ \frac{|\gamma|}{\gamma} E_z^I(x) \end{pmatrix}, \\ \begin{pmatrix} \bar{J}_x(x) \\ \bar{J}_z(x) \end{pmatrix} &= j\omega\mu_0 \begin{pmatrix} J_x(x) \\ \frac{\gamma}{|\gamma|} J_z(x) \end{pmatrix} \end{aligned} \quad (2)$$

which relate the physical field in Region I of Fig. 1 and the current density to the quantities (bar) used in (1) via the purely real or imaginary values of  $\gamma$ . Indeed, no other values of  $\gamma$  are possible which is concluded from the fact that (1) can be interpreted as the limit of the equivalent shielded microstrip equation with sidewalls removed to infinity [10]. By comparison of the impedance terms  $Z_{xx} \cdots Z_{zz}$  with those occurring in an analogous formulation of the uncovered, i.e., open strip problem it can also be seen what happens if the height  $h$  of the conducting cover plate is increased. For all modes propagating with  $\gamma = j\beta$  and  $\beta$  exceeding the wave-number  $k_0\sqrt{\epsilon_{II}}$  of a plane wave in medium II the open and the covered type solutions coincide in the limit of large  $h$ . This for example prevails always in the case of quasi-TEM modes. For values of  $\beta$  smaller than  $k_0\sqrt{\epsilon_{II}}$  or  $\gamma = \alpha$  real the open type equations become complex indicating the existence of leaky modes.

The numerical solution of (1) will now be achieved for single and coupled lines by the method of moments with an optimal choice of expansion and testing functions. First, due to a variational interpretation given by Harrington [15] and the self-adjointness of the integral operator in (1) as a consequence of its symmetry, both types of functions should be equal which means that Galerkin's method [15] has to be applied. The symmetrical matrix ( $A$ ) resulting from this conventional procedure contains elements like

$$A_{ik}^{xz} = \int_0^{N\pi} Z_{xz}(\gamma, K_x) \tilde{f}_{xi}(K_x) \tilde{f}_{zk}(K_x) dK_x, \\ K_x = wk_x, \quad N \rightarrow \infty \quad (3)$$

and the zeros of the corresponding determinant  $\det(\gamma)$  of ( $A$ ) render the required eigenvalues. Back-substitution into  $\det(\gamma)$  then supplies the current distribution and from this subsequently the electromagnetic field may be derived [10]. The terms  $\tilde{f}_{xi}(K_x), \tilde{f}_{zk}(K_x)$  can be recognized as the Fourier

sine and cosine transforms [16] of the transverse and longitudinal current density expansion functions  $f_{xi}(x), f_{zk}(x)$ . These are selected now in accordance with the following criteria.

1) For rapid convergence of the solution they should term by term satisfy the edge condition [17] which requires that  $J_x(x)$  behaves like  $|x - x_e|^{1/2}$  near the edge  $x_e$  of a strip whereas  $J_z(x)$  approaches  $x_e$  with the singularity  $|x - x_e|^{-1/2}$ . This ensures the proper singular behavior of the field for any degree of solution accuracy and is necessary to achieve fast convergence of the characteristic impedance values, which quite sensitively depend on the field distribution. In a similar fashion Silvester and Benedek [18] have treated singularities in electrostatic microstrip problems.

2) In order to avoid the additional numerical expense going along with the existence of extraneous, unphysical solutions like those only recently reported by Farrar and Adams [12]  $f_{xi}(x)$  and  $f_{zk}(x)$  have to be chosen twice continuously differentiable. This has been found empirically as the result of test computations with various kinds of expansion functions, among others pulse-functions, polynomials, finite-element-polynomials of orders one to three, spline functions (continuous first derivative), Fourier series expansions with and without edge terms [10]. Spurious solutions were detected only in cases where the above condition was violated. Surely, continuity of the first two derivatives is a physical property of the surface current density and it should therefore be included *a priori* for reasons of convergence. Furthermore, since the process of deriving the integral equation (1) involves an extension of the originally underlying Helmholtz operator, the use of expansion functions which are discontinuous or have discontinuous derivatives, i.e., outside the original domain, is most probably the cause of extraneous solutions (see [15]) like the above.

3) The system of functions  $f_{xi}, f_{zk}$  should be complete to enable approximation of the exact solution to any degree of accuracy by simply increasing the upper summation limit  $i_{\max}$  of the expansion. In this way the numerical solutions can be easily checked for their grade of convergence.

4) In view of the special kind of  $x$ -dependence which the  $x$  and the  $z$  component of the magnetic field at  $y = 0$  exhibit due to deduction from the same electromagnetic potentials [10] it has turned out advantageous to introduce an integral relationship between the functions  $f_{xi}(x)$  and  $f_{zi}(x)$  corresponding in their subscripts  $i$ . This is consistent with the symmetry properties (even-odd) of the current components and also with their edge behavior. In addition, since this means relating the transforms  $\tilde{f}_{xi}(K_x)$  and  $\tilde{f}_{zi}(K_x)$  by simply a factor of  $K_x$  the CP-time necessary for generating one of these transforms and also considerable storage is saved. Moreover, introducing the auxiliary spectral function

$$\tilde{g}_i(K_x) = \tilde{f}_{zi}(K_x)/\sqrt{K_x} = \tilde{f}_{xi}(K_x) \cdot \sqrt{K_x} \quad (4)$$

leads to a symmetrization of the matrix elements (3) and thus further reduces time requirements. In the limit of large values of  $i_{\max}$  only 37.5 percent of the matrix ( $A$ ) is non-redundant information due to its high degree of symmetry.

5) All the physical insight gained from earlier computations should be incorporated into the choice of the expansion functions so that every pair  $i$  of them can nearly represent a modal current distribution and the matrix size can be held small for a given required solution accuracy.

6) Besides the above more physical requirements at the same time numerical aspects have to be taken into account. These demand that the transforms  $\tilde{f}_{xi}, \tilde{f}_{zi}$  are available in a not-too-complicated analytical form and that the final matrix  $(A)$  is well conditioned [15], [19]. None of the recent authors [1]–[12] has applied these criteria altogether. In fact, some of them use rather poorly behaved expansion functions which seem hardly suited for the computation of quantities reacting more sensitively to a bad choice than the propagation constants. Therefore, as an optimal set of current density basis functions with regard to the above criteria for the even modes ( $E$ ) on single microstrip lines it is here proposed

$$\begin{aligned} f_{z0}^E(X) &= 1/\sqrt{1-X^2} \\ f_{zi}^E(X) &= (\cos(i\pi X) - B_0(i\pi))/\sqrt{1-X^2} \\ f_{x0}^E(X) &\equiv 0 \\ f_{xi}^E(X) &= \int_0^X f_{zi}^E(X') dX', \quad 0 \leq X < 1 \end{aligned} \quad (5)$$

with  $i = 1, 2, \dots, \infty$  and the variable  $X$  running from 0 at the middle of the strip to 1 at the edge. In the transform domain this yields

$$\begin{aligned} \tilde{f}_{z0}^E(K_x) &= 2B_0(K_x) \\ \tilde{f}_{zi}^E(K_x) &= B_0(K_x - i\pi) + B_0(K_x + i\pi) - 2B_0(i\pi)B_0(K_x) \\ \tilde{f}_{x0}^E(K_x) &\equiv 0 \\ \tilde{f}_{xi}^E(K_x) &= \tilde{f}_{zi}^E(K_x)/K_x, \quad 0 \leq K_x < \infty. \end{aligned} \quad (6)$$

In both equations  $B_0$  denotes the zero order Bessel function of the first kind. The term  $f_{z0}^E(X)$  describes the charge density distribution of a strip in free space and has often been used for approximate fundamental mode solutions, for example by Denlinger [20]. Similarly, for the odd modes ( $O$ ) on a single line an expansion is used with the elements

$$\begin{aligned} f_{xi}^O(X) &= \cos(i\pi X) \cdot \sqrt{1-X^2}, \\ f_{zi}^O(X) &= df_{xi}^O(X)/dX, \\ \tilde{f}_{xi}^O(K_x) &= B_1(K_x - i\pi)/(K_x - i\pi) + B_1(K_x + i\pi)/(K_x + i\pi), \\ \tilde{f}_{zi}^O(K_x) &= K_x \cdot \tilde{f}_{xi}^O(K_x) \end{aligned} \quad (7)$$

and with  $i$  from zero to infinity.  $B_1$  stands for the first-order Bessel function.

Regarding the even and odd modes on coupled microstrip lines one has to bear in mind that in case of wide spacings  $s$  solutions similar to those existing on two decoupled single lines have to be expected. Especially, now two quasi-TEM modes exist which in the limit of large  $s$  result in the same fundamental mode on two single strips with a difference only

in the state of phase. For this reason the even and odd mode sets of coupled line basis functions are both derived in analogy to (5), (6). They shall not be given explicitly here. That the proposed functions are surely an optimum set can be seen from the fact that each pair  $i$  of them (together with the zero order term for even modes) indeed turns out to approximate a modal solution, as is obvious from an example in the results section. With this property convergence must be rapid once the number  $i_{\max}$  of expansion terms exceeds the mode number  $i$ , which is, however, only one aspect of numerical efficiency. The other aspect concerns the numerical expense necessary to generate the eigenvalue equations. Here, especially the fourth criterion provides a reduction together with the normalization (2). Independent of the choice of basis functions splitting up the matrix  $(A)$  into the product of a diagonal matrix  $(Z)$  and a matrix  $(G)$  which contains the frequency independent structural information brings further advantage [10]. Comparative test runs which partially or altogether did not take care of the described criteria and computational details resulted in CP-times which were higher by a factor of 3–100 (0.5-percent numerical accuracy of the characteristic impedance). This clearly confirms Harrington [15] who regards the choice of the expansion functions as one of the main tasks in any particular problem.

## RESULTS

The computations described in this paper were performed on a Control Data 6400 of the Technical University of Aachen computer center. Unless otherwise noted the results all refer to an alumina substrate with the following specifications: Dielectric constant  $\epsilon_r = 9.9$ , dielectric loss tangent  $\tan \delta = 0.0005$ , substrate thickness  $d = 0.64$  mm and rms surface roughness  $d_{SR} = 0.25 \mu\text{m}$ . The copper metallization deposited on this substrate is  $t = 5 \mu\text{m}$  thick and has a resistivity of  $\rho = 18 \times 10^{-6} \Omega\text{mm}$ . Whenever the cover height  $h$  is not given explicitly a choice of  $h = 10^7$  m, i.e., the case of open microstrip prevails. The space above the substrate is filled with air. The frequency region of interest is 0–16 GHz.

Since the above computations do not contain the effect of finite strip thickness this has been introduced supplementarily for the quasi-TEM modes. In view of the small percentage influence of  $t$  except for impractically small strip widths and spacings [21], [22] the excess work involved in a rigorous solution of the finite thickness strip boundary value problem can surely not be justified for design purposes. Therefore, for the single microstrip nonzero values of  $t$  have been taken into account by a modification of the strip width  $w$  to  $w_t$  which is given by Hammerstad and Bekkadal [22] as

$$\begin{aligned} w_t &= w + \Delta w = w + t \cdot (1 + \ln(2d/t))/\pi, \\ &\quad w > d/2\pi > 2t \\ w_t &= w + \Delta w = w + t \cdot (1 + \ln(4\pi w/t))/\pi, \\ &\quad d/2\pi > w > 2t. \end{aligned} \quad (8)$$

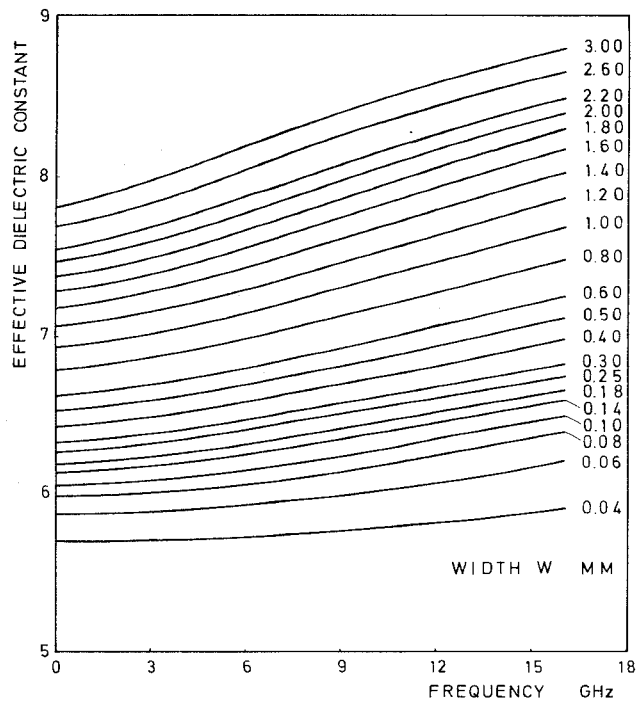


Fig. 2. Frequency dependent effective dielectric constant of the quasi-TEM mode on single microstrip lines.

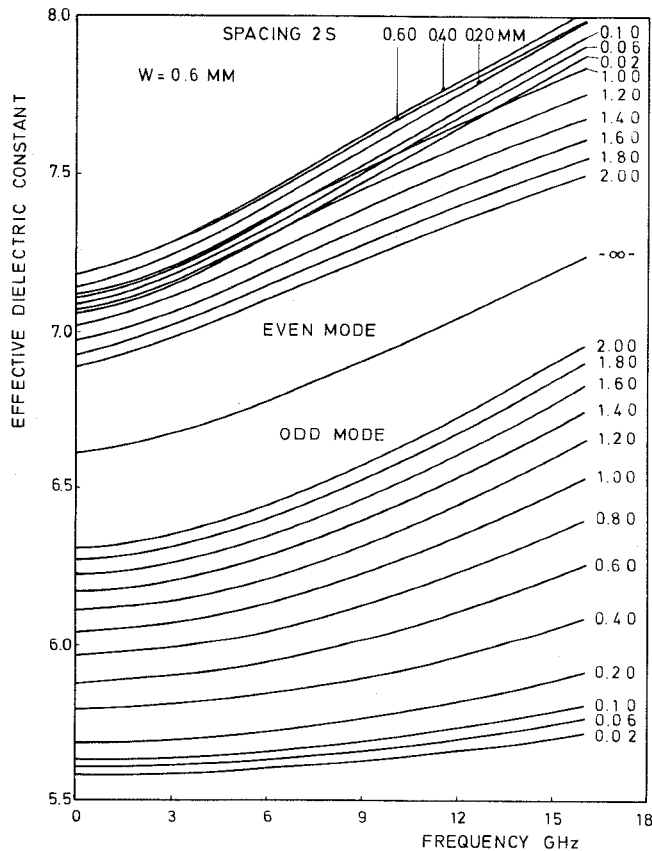


Fig. 3. Frequency dispersion of the even and odd quasi-TEM mode on coupled microstrip lines for a fixed width of  $w = 0.6$  mm and varying spacings.

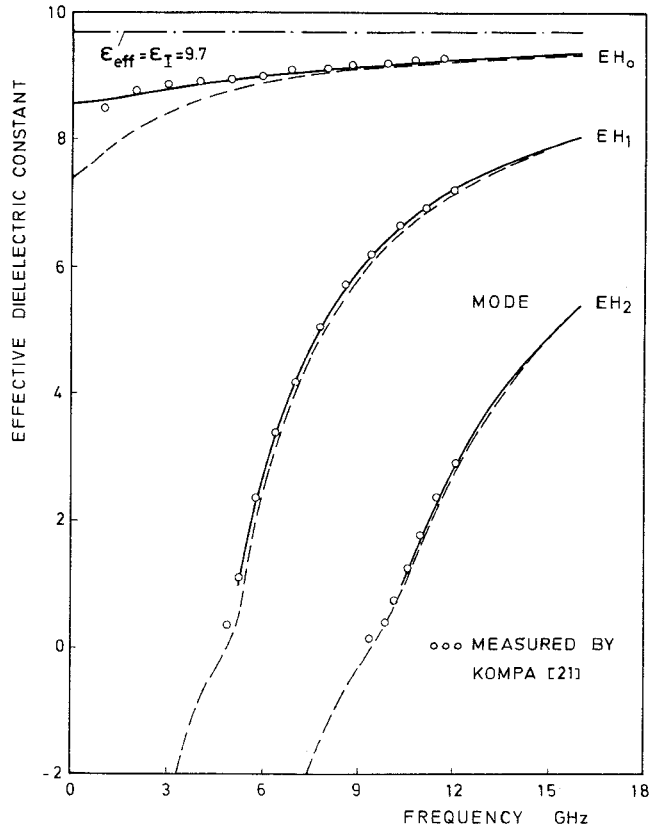


Fig. 4. Dispersion characteristics of the fundamental and the first two higher order modes on a wide single microstrip line ( $\epsilon_I = 9.7$ ,  $w = 9.15$  mm), dashed curve: cover height  $h = 3d = 1.92$  mm.

Similarly, for coupled microstrip lines and in the range of technologically meaningful geometries useful corrected strip width values have been found to be

$$w_t^E = w + \Delta w \cdot (1 - 0.5 \exp(-0.69\Delta w/\Delta t)),$$

$$\Delta t = t \cdot d \cdot \epsilon_{II}/(s \cdot \epsilon_I)$$

$$w_t^O = w + \Delta w \cdot (1 - 0.5 \exp(-0.69\Delta w/\Delta t)) + \Delta t,$$

$$s \gg 2t \quad (9)$$

where  $E$  again indicates the even and  $O$  the odd mode case.  $\Delta t$  is the increase in strip width necessary to approximately describe the additional odd mode coupling capacitance arising from nonzero strip thickness. At the same time  $\Delta w/\Delta t$  serves as a relative measure of distance from the symmetry plane  $x = 0$ . For large spacings  $s$  the single line formula (8) results.

As a first proof of the efficiency of the calculation method under discussion the fundamental mode ( $EH_0$ ) frequency dispersion charts Fig. 2 and Fig. 3 have been generated. The effective dielectric constant  $\epsilon_{eff}$  appearing in these and other plots is defined in the usual way as  $-(\gamma/k_0)^2$  with  $k_0$  denoting the free-space wavenumber. Test measurements like those in [10] throughout have revealed a coincidence of better than 1 percent for various widths and spacings. The CP-time necessary to compute one point of Fig. 2 is approximately 0.25 s for a numerical accuracy of better than 0.1 percent (first-order solution,  $i_{max} = 1$ , matrix order 3). In all practical applications 0.3 percent is accurate

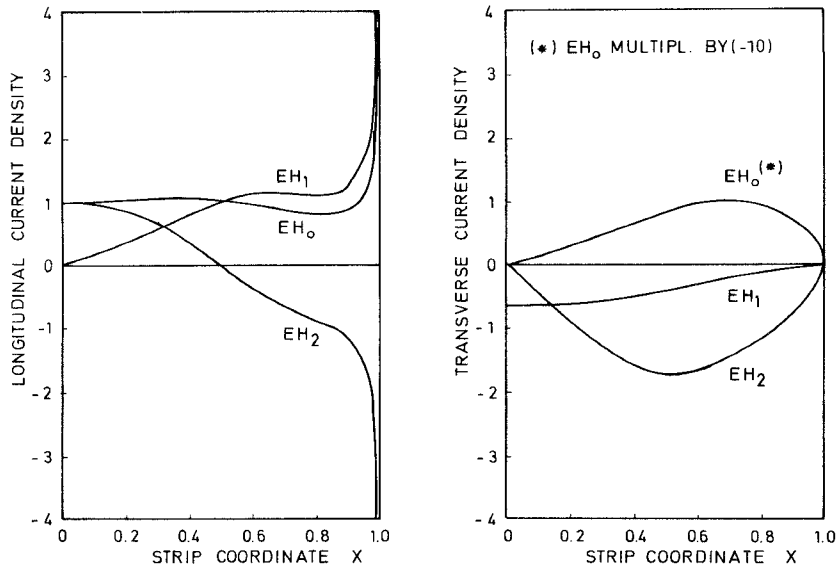


Fig. 5. Normalized modal strip current density components of the first three modes on a wide single microstrip line at a frequency of 12 GHz ( $\epsilon_1 = 9.7$ ,  $w = 9.15$  mm).

enough and the zero order solution with less than 0.10 s CP-time per point is sufficient. Except for very small spacings where  $i_{\max} = 2$  has been applied this is also valid for the generation of Fig. 3. Due to the partitioning into even and odd solutions time consumption for the single line first higher order mode  $EH_1$  is very similar too. So, charts like these can be provided for broad-band design purposes with little cost. Their physical interpretation will not be given here. As an interesting fact, however, the nonmonotonical behavior of the even mode with respect to the line spacing in Fig. 3 shall be mentioned. This is due to the fact that for very small spacings the even mode cannot form a noticeable fringing field between the lines. So, an increase of  $s$  then appears as an increase of the overall width  $2w + 2s$  and is accompanied by a higher value of  $\epsilon_{\text{eff}}$ .

Higher order modes on a wide single microstrip line and the associated modal current distributions have been computed in Fig. 4 and Fig. 5. For comparison with open line measurements made by Kompa [23] there a slightly different substrate dielectric constant of  $\epsilon_1 = 9.7$  is considered. The coincidence exhibited by Fig. 4 is excellent for all modes. The dashed curves which for the higher order solutions go down into the attenuation region refer to a cover height of  $h = 3d = 1.92$  mm. They show that for flat packages, i.e., small values of  $h$ , the frequency dispersion of the quasi-TEM ( $EH_0$ ) mode is rapidly increased in the low gigahertz range. Modal normalized current density solutions corresponding to Fig. 4 (open line) at 12 GHz are depicted in Fig. 5 with the relative magnitude of the transverse and longitudinal components conserved.  $X = 0$  is the strip middle. As a consequence of the criteria incorporated into the expansion functions the solutions are smoothly curved and highly accurate though only a matrix of order 7 ( $i_{\max} = 3$ ) has been involved in their computation.

Further results to be given in Fig. 6 and Fig. 7 are charts of the frequency dependent characteristic impedance  $Z_L$  of the

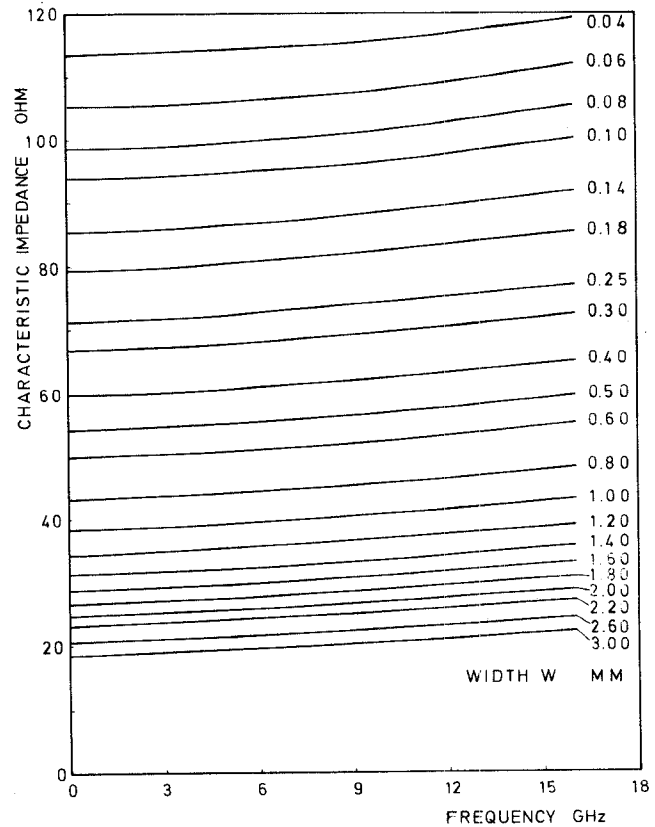


Fig. 6. Single microstrip quasi-TEM characteristic impedance as a function of frequency.

fundamental modes on single and coupled microstrip lines. The quantity  $Z_L$  shown there is defined on a voltage per longitudinal current basis with the voltage  $U$  equal to the line integral over the electric field from the strip middle perpendicular to the ground. This definition instead of one of two other possible ones [13] has been chosen for reasons of numerical efficiency. In fact, generation of the character-

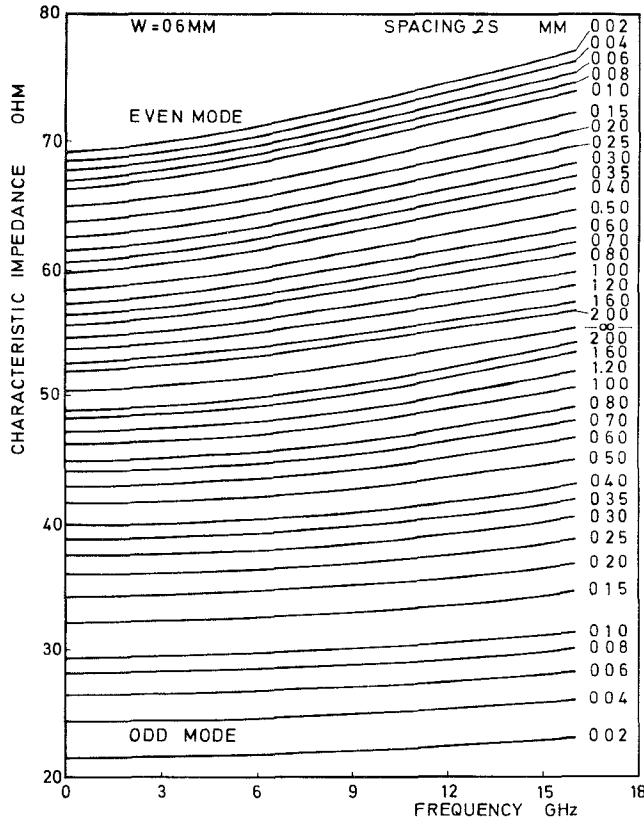


Fig. 7. Frequency dependent characteristic impedance of the even and odd quasi-TEM mode on coupled microstrip lines for a fixed width of  $w = 0.6$  mm and varying spacings.

istic impedance in addition to the effective dielectric constant increases CP-time by only a small fraction. However, the mean 1.0-percent numerical accuracy in Figs. 6 and 7 is less than that of the corresponding diagrams Figs. 2 and 3. This verifies the assumption of Knorr and Tufekcioglu [13] that the voltage  $U$  reacts sensitively to an assumed distribution of surface current. It should be noted therefore that the zeroth-order expansion of this paper is already equivalent to the improved distribution proposed in [13].

Another quantity which is useful in the modeling of microstrip lines is the effective width  $w_{\text{eff}}$  [23], namely the width of an equivalent parallel-plate waveguide of height  $d$  and with the microstrip values of  $Z_L$  and  $\beta$ .  $w_{\text{eff}}$  may at the same time be interpreted as a measure of noticeable field extension away from a strip or likewise as the effective width of the current density path on the ground plane. Its dependence on the actual strip width  $w$  of a single microstrip line is depicted in Fig. 8. Due to the relation

$$w_{\text{eff}}/w = Z_0 \cdot d / (Z_L \cdot \sqrt{\epsilon_{\text{eff}}}), \quad Z_0 = 120\pi\Omega \quad (10)$$

the decrease of the  $w_{\text{eff}}$  with frequency is the accumulated increase of  $Z_L$  and the square-root of  $\epsilon_{\text{eff}}$ .

Finally, loss calculations for the fundamental modes which also do not substantially prolong the reported CP-times shall be presented in Figs. 9 and 10. The knowledge of total loss  $\alpha_{\text{tot}}$  beyond that of frequency dispersion or equivalently the knowledge of the quality factor  $Q = \beta/2\alpha$  is for example important in the design of filters and couplers [24].

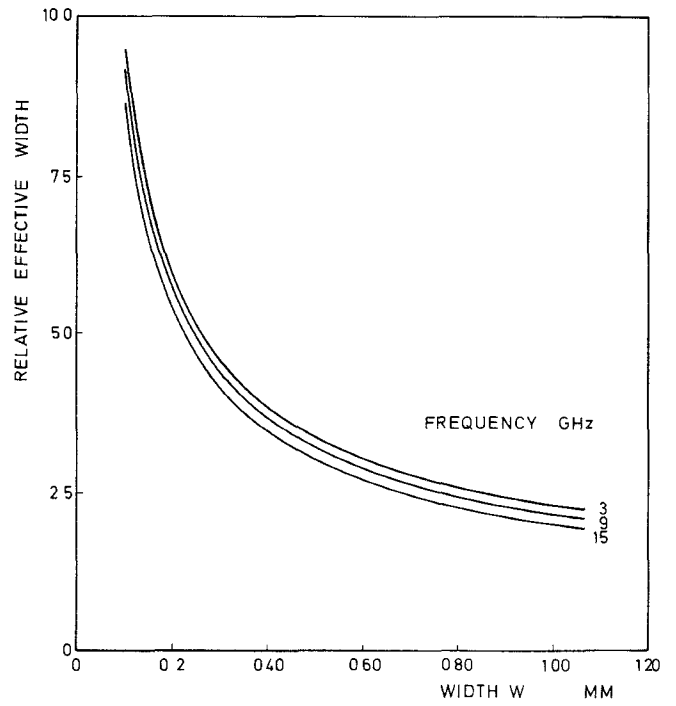


Fig. 8. Relative effective width  $w_{\text{eff}}/w$  of the parallel-plate waveguide equivalents of single microstrip lines.

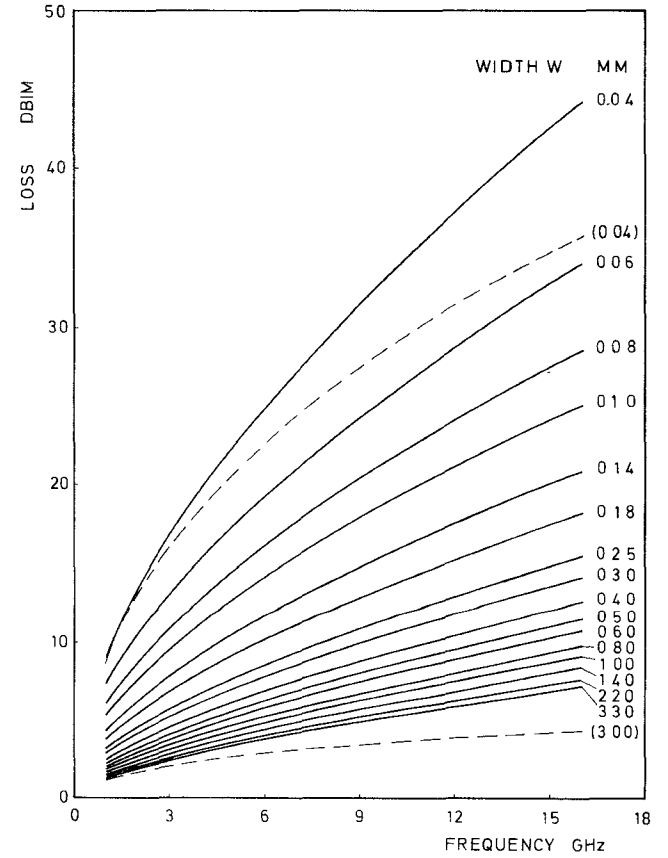


Fig. 9. Total loss of single microstrip lines on alumina, dashed curves: conduction loss without effect of substrate surface roughness.

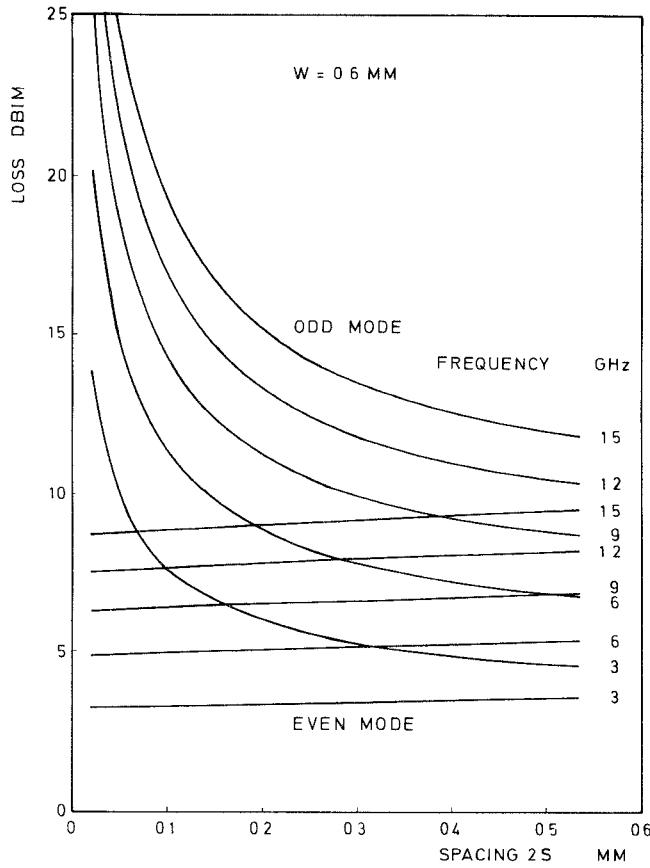


Fig. 10. Total loss of coupled microstrip lines on alumina for a fixed width of  $w = 0.6$  mm and varying spacings.

Its evaluation starts here from the conventional transmission line formula

$$\alpha_{\text{tot}} = \alpha_{\text{cond.}} + \alpha_{\text{dielectric}} = 0.5R'/Z_L + 0.5k_0 \cdot \sqrt{\epsilon_{\text{eff}}} \cdot \tan \delta \quad (11)$$

with the line resistance per unit length  $R'$  in (11) calculated according to the relation

$$R' = (R_s/w_{\text{eff}} + F_J \cdot R_s/w_t) \cdot F_{SR},$$

$$F_J = \int_0^1 |\bar{J}_z(X)|^2 dX / \left( \int_0^1 \bar{J}_z(X) dX \right)^2 \quad (12)$$

and  $R_s$  denoting the surface skin resistivity. In (12) which is only valid for not too low frequencies the first term accounts for conduction loss on the ground plane. The second one describes loss originating from the lower side and the sidewalls of a strip and is an appreciably higher term except for very wide lines. Current flow on the upper side of the strip conductor has been neglected so that for small line widths the value of  $R'$  should be a bit too high. This is, however, not serious since in practical circuits radiation loss caused by statistical irregularities of the line cross section arises which is not considered here and which also grows for smaller widths. The increase of strip loss due to the nonuniform current distribution compared with a uniform one is represented by the factor  $F_J$  [25].  $F_J$  results from the eigen-solutions by numerical integration and under consideration of the edge singularity of the strip of finite thickness

(rectangular bar on dielectric, see [17]). For single microstrips and in the range of widths as given in Fig. 2 it varies between about 1.35–1.15 approaching 1.00 in the parallel plate limit  $w \gg d$ . In agreement with the calculations made by Horton [26] and as visible in Fig. 10 tightly coupled lines may exhibit large values of  $F_J$  for the odd quasi-TEM mode. A further factor denoted  $F_{SR}$  is provided by Hammerstad and Bekkadal [22] and describes the additional loss due to substrate surface roughness. According to (11) all these contributions are incorporated into the charts Fig. 9 and Fig. 10. The dashed curves in Fig. 9 only serve for comparison and do neither include surface roughness nor dielectric loss. Their deviation from the corresponding solid line curve is mainly the effect of neglection of roughness for the narrow line and of  $\tan \delta$  for the wide one. The accuracy of the loss calculations Figs. 9 and 10 should be adequate for most practical purposes.

## CONCLUSION

A high speed numerical solution of the hybrid mode problem of single and coupled microstrip lines has been presented. Based thereon frequency dependent microstrip design data have been calculated with up to now unknown computational efficiency. The procedure may easily be extended to more complicated strip patterns [14].

## ACKNOWLEDGMENT

Thanks are due to Prof. Dr.-Ing. H. Döring who encouraged and supported this work.

## REFERENCES

- [1] R. Mittra and T. Itoh, "A new technique for the analysis of the dispersion characteristics of microstrip lines," *IEEE Trans. Microwave Theory Tech.*, vol. MTT-19, pp. 47–56, Jan. 1971.
- [2] M. K. Krage and G. I. Haddad, "Frequency-dependent characteristics of microstrip transmission lines," *IEEE Trans. Microwave Theory Tech.*, vol. MTT-20, pp. 678–688, Oct. 1972.
- [3] A. R. Van de Capelle and P. J. Luypaert, "Fundamental- and higher-order modes in open microstrip lines," *Elecron. Letts.*, vol. 9, pp. 345–346, July 1973.
- [4] T. Itoh and R. Mittra, "Spectral-domain approach for calculating the dispersion characteristics of microstrip lines," *IEEE Trans. Microwave Theory Tech.*, vol. MTT-21, pp. 496–499, July 1973.
- [5] R. H. Jansen, "A modified least-squares boundary residual (LSBR) method and its application to the problem of shielded microstrip dispersion," *Electronics and Communication (AEÜ)*, vol. 28, pp. 275–277, June 1974.
- [6] T. Itoh and R. Mittra, "A technique for computing dispersion characteristics of shielded microstrip lines," *IEEE Trans. Microwave Theory Tech.*, vol. MTT-22, pp. 896–898, Oct. 1974.
- [7] R. H. Jansen, "A moment method for covered microstrip dispersion," *Electronics and Communication (AEÜ)*, vol. 29, pp. 17–20, Jan. 1975.
- [8] —, "Computer analysis of edge coupled planar structures," *Elecron. Letts.*, vol. 10, pp. 520–522, Nov. 1974.
- [9] —, "Computer analysis of shielded microstrip structures" (in German). *Electronics and Communication (AEÜ)*, vol. 29, pp. 241–247, June 1975.
- [10] —, "Numerical computation of the eigenfrequencies and eigenfunctions of arbitrarily shaped microstrip structures" (in German), Ph.D. dissertation, Aachen Tech. Univ., Germany, June 1975.
- [11] E. Yamashita and K. Atsuki, "Analysis of microstrip-like transmission lines by nonuniform discretization of integral equations," *IEEE Trans. Microwave Theory Tech.*, vol. MTT-24, pp. 195–200, Apr. 1976.
- [12] A. Farrar and A. T. Adams, "Computation of propagation constants

for the fundamental and higher order modes in microstrip," *IEEE Trans. Microwave Theory Tech.*, vol. MTT-24, pp. 456-460, July 1976.

[13] J. B. Knorr and A. Tufekcioglu, "Spectral-domain calculation of microstrip characteristic impedance," *IEEE Trans. Microwave Theory Tech.*, vol. MTT-23, pp. 725-728, Sept. 1975.

[14] R. H. Jansen, "Fast accurate hybrid mode computation of nonsymmetrical coupled microstrip characteristics," presented at 7th European Microwave Conference, Feb. 1977.

[15] R. F. Harrington, *Field Computation by Moment Methods*. New York: Macmillan, 1968, secs. 1-8, 1-7, 7-6, 1-3.

[16] I. N. Sneddon, *The Use of Integral Transforms*. New Delhi, India: Tata McGraw-Hill, 1974, pp. 42-46.

[17] R. Mittra and S. W. Lee, *Analytical Techniques in the Theory of Guided Waves*. New York: Macmillan, 1971, pp. 4-11.

[18] P. Silvester and P. Benedek, "Electrostatics of the microstrip-revisited," *IEEE Trans. Microwave Theory Tech.*, vol. MTT-20, pp. 756-758, Nov. 1972.

[19] J. R. Westlake, *A Handbook of Numerical Matrix Inversion and Solution of Linear Equations*. New York: Wiley, 1968, pp. 88-91.

[20] E. J. Denlinger, "A frequency dependent solution for microstrip transmission lines," *IEEE Trans. Microwave Theory Tech.*, vol. MTT-19, pp. 30-39, Jan. 1971.

[21] G. Kowalski and R. Pregla, "Dispersion characteristics of shielded microstrip with finite thickness," *Electronics and Communications (AEÜ)*, vol. 25, pp. 193-196, Apr. 1971.

[22] E. O. Hammerstad and F. Bekkadal, "Microstrip handbook," ELAB Rep. STF 44 A 74169, Univ. Trondheim, Norway, Feb. 1975.

[23] G. Kompa, "The frequency dependent transmission properties of microstrip impedance steps, filters and stubs" (in German), Ph.D. dissertation, Aachen Tech. Univ., Germany, May 1975.

[24] B. Rama Rao, "Effect of loss and frequency dispersion on the performance of microstrip directional couplers and coupled line filters," *IEEE Trans. Microwave Theory Tech.*, vol. MTT-22, pp. 747-750, July 1974.

[25] S. Ramo and J. R. Whinnery, *Fields and Waves in Modern Radio*. New York: Wiley, 1953.

[26] R. Horton, "Loss calculations of coupled microstrip lines," *IEEE Trans. Microwave Theory Tech.*, vol. MTT-21, pp. 359-360, May 1973.

# A Simple Method for Determining the Green's Function for a Large Class of MIC Lines Having Multilayered Dielectric Structures

RAYMOND CRAMPAGNE, MAJID AHMADPANAH, AND JEAN-LOUIS GUIRAUD

**Abstract**—To find the characteristic parameters of the wave propagation in microstrip structures, several Green's function methods have already been developed, corresponding to particular geometric configurations. In this paper, three of these methods are synthesized, showing that the final equations in the different cases are identical. Moreover, using the transverse transmission line theory, the Green's function is solved numerically for an  $N$ -layer dielectric structure.

## I. INTRODUCTION

MICROSTRIP transmission lines are largely used in the microwave integrated circuits. Although being a simplifying approximation, the quasi-TEM approximation is well known to have proved useful in giving quite accurate results for practical purposes. The characteristic parameters

of such lines have been calculated, using various methods. The method utilizing Green's potential function lets one transform a differential equation to an integral one; where the unknown quantity becomes the charge density. This is solved easily by numerical techniques using the moment and the point matching methods.

In this method, the conductor geometry can be defined exactly; in particular the conductor's thickness and the dissymmetry in the strip configuration can be taken into account. However, we assume infinitely thin symmetric conductors because these parameters do not modify the determination of the Green's function.

The present paper tries to generalize the studies done on microstrip lines with two or three layers of dielectric [1]-[3] in that it determines the Green's function for multilayer microstrip lines having the same conductor geometry as used in previous studies. Our main aim had been at presenting the results in analytic form which lends itself to numeric solution, requiring very little modification in the programs already existing.

Manuscript received January 13, 1977; revised April 5, 1977.

R. Crampagne and M. Ahmadpanah are with Laboratoire de Microondes, 2, rue Camichel—31 071 Toulouse, France.

J. L. Guiraud is with Laboratoire de Physique Mathématique, 118, route de Narbonne—31 077 Toulouse, France.